


Leukemia (2018) 32:1435–1444  
<https://doi.org/10.1038/s41375-018-0085-1>

## ARTICLE



## Animal models

# Tracking preleukemic cells in vivo to reveal the sequence of molecular events in radiation leukemogenesis

Tom Verbiest<sup>1,2</sup> · Rosemary Finnon<sup>1</sup> · Natalie Brown<sup>1</sup> · Lourdes Cruz-Garcia<sup>1</sup> · Paul Finnon<sup>1</sup> · Grainne O'Brien<sup>1</sup> · Eleanor Ross<sup>3</sup> · Simon Bouffler<sup>1</sup> · Cheryl L. Scudamore<sup>3</sup> · Christophe Badie<sup>1</sup> 

Received: 6 October 2017 / Revised: 5 February 2018 / Accepted: 6 February 2018 / Published online: 3 March 2018  
 © The Author(s) 2018. This article is published with open access

**Abstract**

Epidemiological studies have demonstrated an increased leukemia incidence following ionizing radiation exposure, but to date, the target cells and underlying mechanisms of radiation leukemogenesis remain largely unidentified. We engineered a mouse model carrying a different fluorescent marker on each chromosome 2, located inside the minimum deleted region occurring after radiation exposure and recognized as the first leukemogenic event. Using this tailored model, we report that following radiation exposure, more than half of asymptomatic CBA *Sfpil*<sup>GFP/mCh</sup> mice presented with expanding clones of preleukemic hematopoietic cells harboring a hemizygous interstitial deletion of chromosome 2. Moreover, following isolation of preleukemic hematopoietic stem and progenitor cells irradiated in their native microenvironment, we identified the presence of *Sfpil* point mutations within a subpopulation of these preleukemic cells expanding rapidly (increasing from 6% to 55% in 21 days in peripheral blood in one case), hence identifying for the first time the presence of such cells within a living animal. Importantly, we also report a previously undescribed gender difference in the phenotype of the preleukemic cells and leukemia, suggesting a gender imbalance in the radiation-induced leukemic target cell. In conclusion, we provide novel insights into the sequence of molecular events occurring during the (radiation-induced) leukemic clonal evolution.

**Introduction**

It is widely recognized that exposure to ionizing radiation increases leukemia incidence [1–6]. Radiation leukemogenesis is a genetically complex, multistep process, and the underlying mechanisms and target cells remain unidentified [7]. The CBA inbred mouse strain is a model of radiation-induced acute myeloid leukemia (rAML) [8, 9] where hemizygous interstitial deletion of chromosome

2 (Del2) is a characteristic finding [10] with the minimal deleted region (MDR) containing *Sfpil*, encoding the hematopoietic transcription factor PU.1 [11]. In ~85% of the cases, the remaining *Sfpil* copy carries a point mutation in a single CGC codon, within the DNA binding domain in exon 5 [12]. These biallelic *Sfpil* aberrations support a two-hit model in murine rAML [13]. Bone marrow (BM) cells carrying Del2 can be identified 24 h post-irradiation, and it is assumed that Del2 HSPCs expand clonally [14]. Ultimately, 15–20% of mice will present with AML [15].

All data generated previously used fixed leukemic cells to study Del2 and *Sfpil* mutations, thus limiting further characterization of leukemogenesis. Here, we crossed CBA *Sfpil*<sup>GFP/GFP</sup> mice [16] with a newly generated CBA *Sfpil*<sup>mCh/mCh</sup> transgenic model to create an F1 CBA *Sfpil*<sup>mCh/GFP</sup> mouse expressing mCherry from a Rosa26 promoter construct located in the chromosome 2 MDR, and GFP being expressed from the other allele under the *Sfpil* promoter. Monthly blood sampling post-irradiation was used to monitor Del2, and preleukemic clonal expansion, by flow cytometry.

We report that more than half of mice presented with preleukemic cells harboring Del2. Moreover, we identified

**Electronic supplementary material** The online version of this article (<https://doi.org/10.1038/s41375-018-0085-1>) contains supplementary material, which is available to authorized users.

✉ Christophe Badie  
[christophe.badie@phe.gov.uk](mailto:christophe.badie@phe.gov.uk)

- <sup>1</sup> Cancer Mechanisms and Biomarkers Group, Radiation Effects Department, Centre for Radiation, Chemical and Environmental Hazards, Public Health England, Didcot OX11 0RQ, UK
- <sup>2</sup> CRUK & MRC Oxford Institute for Radiation Oncology, Department of Oncology, University of Oxford, Oxford OX3 7DQ, UK
- <sup>3</sup> Mary Lyon Centre, MRC Harwell, Oxfordshire OX11 0RD, UK

for the first time the presence of *Sfp1* point mutations within subpopulations of these preleukemic cells, within a living animal. We also provide evidence of a gender difference in the (pre)leukemic phenotype, suggesting a difference in the leukemic target cell between male and female mice.

## Methods

### Mice, rAML induction, and tissue preparation

CBA *Sfp1*<sup>mCh/mCh</sup> mice were generated as previously described [17], and mated to CBA *Sfp1*<sup>GFP/GFP</sup> mice [16] to generate F1 CBA *Sfp1*<sup>mCh/GFP</sup> mice. Mice were given single 3Gy whole-body X-irradiation at 10–12 weeks of age (70 males and 50 females). Sham-irradiation of age-matched mice ( $n = 20$ ; assigned at random) was performed by placing the mice into the irradiator box for the appropriate time without X-rays being produced. rAMLs were diagnosed as described previously [16], using the criteria of the ‘Bethesda proposals for classification of nonlymphoid neoplasms in mice’ [18]. Spleen tissue was stored at  $-70^{\circ}\text{C}$  in RNAlater® (Ambion, Austin, US) for nucleic acid extraction, in 4% formaldehyde for histopathological analysis, or disaggregated for FACS analysis, as described previously [16]. All animal procedures conformed to the UK Animals (Scientific Procedures) Act, 1986, Amendment Regulations 2012, and animal experimental protocols were reviewed and approved by the local Ethics Committee and the Home Office.

### Immunophenotyping of leukemic spleen cells

Spleen cells were incubated with phycoerythrin (PE)-conjugated antibodies: Sca1 (E13-161.7; BioLegend), cKit (2B8; Abcam, Cambridge, UK), Flt3 (A2F10.1), Gr1 (1A8), Ly6c (HK1.4; Abcam), Mac1 (M1/70), CD31 (MEC13.3), CD3 (17A2), and B220 (RA3-6B2). All reagents were purchased from BD Biosciences, unless otherwise stated. Acquisition was performed using a Guava® easyCyte Single Sample flow cytometer, and analyzed using InCyte™ software (Merck Millipore, Watford, UK).

### DNA isolation from spleens and sequencing for *Sfp1* exon 5 point mutation

DNA was extracted from spleen tissue using a DNeasy® Blood & Tissue kit (Qiagen, Manchester, UK). Exon 5 mutations in *Sfp1* were determined by DNA sequencing as described previously [19, 20], using primer sequences forward 5'-CGACATGAAGGACAGCATCT-3' and reverse 5'-TTTCTTCACCTCGCCTGTCT-3' (IDT, Leuven, Belgium).

### PCR for mCherry and GFP construct detection

Detection of GFP construct was performed as previously described [16]. For detection of the mCherry construct, primer sequences were Cel1-F 5'-GTGACTCCCAACATCTGCCT-3', Cel1-R 5'-CTGCTTGCTTGCAGACTGAG-3', Donor-F3 5'-AAGGGCGAGGAGGATAACAT-3' and Donor-R3 5'-CTTCAGCTTCAGCCTCTGCT-3' (IDT).

### Immunomagnetic cell separation and fluorescence-activated cell sorting

Lin<sup>-</sup> cells were selected using EasySep™ Mouse Hematopoietic Progenitor Cell Enrichment Kit (Stem Cell Technologies, Grenoble, France) and incubated with the following antibodies conjugated with PE, PE-Cy5, PE-Cy7, fluorescein isothiocyanate (FITC), allophycocyanin (APC) or APCeFluor®780: Sca1 (D7), cKit (2B8), CD48 (HM48-1), CD127 (A7R34), and CD150 (TC15-12F12.2; BioLegend, San Diego, USA). All reagents were purchased from Affymetrix (High Wycombe, UK), unless otherwise stated. Flow cytometry acquisition and sorting was performed using MoFlo XDP (Beckman Coulter, High Wycombe, UK).

### Pyrosequencing analysis

DNA was extracted from blood (10  $\mu\text{l}$ ) using DNeasy® kit (Qiagen). Ten ng of DNA was used to amplify the target sequence of *Sfp1* exon 5 by PCR with primer biotinylated forward 5'-GCATCCAGAAGGGCAACC-3' and reverse 5'-TCGCCTGTCTTGCCGTAGT-3' primers generating a 79 bp PCR product. Primers, DNA and PyroMark PCR master mix (Qiagen) were combined in a total volume of 25  $\mu\text{l}$ , and amplified: 15 min at  $95^{\circ}\text{C}$ , then 45 cycles of (30 s at  $95^{\circ}\text{C}$ , 30 s at  $60^{\circ}\text{C}$  and 30 s at  $72^{\circ}\text{C}$ ). Ten  $\mu\text{l}$  of the biotinylated PCR product was used to detect mutations on the first base of the 235th codon (CGC to TGC) with the following sequencing primer: 5'-CCTGTCTTGCCGTAGT-3' using PyroMark48 (Qiagen).

## Results

### Clonal expansion of Del2 hematopoietic cells following radiation exposure

Mice received 3Gy whole-body X-irradiation and underwent monthly tail vein bleeding for lifespan to identify leukocytes carrying Del2, indicated by fluorescence loss (Supplementary Figure S1A). In sham-irradiated mice, all leukocytes expressed mCherry. GFP expression is controlled by PU.1 promoter, hence lymphocytes did not

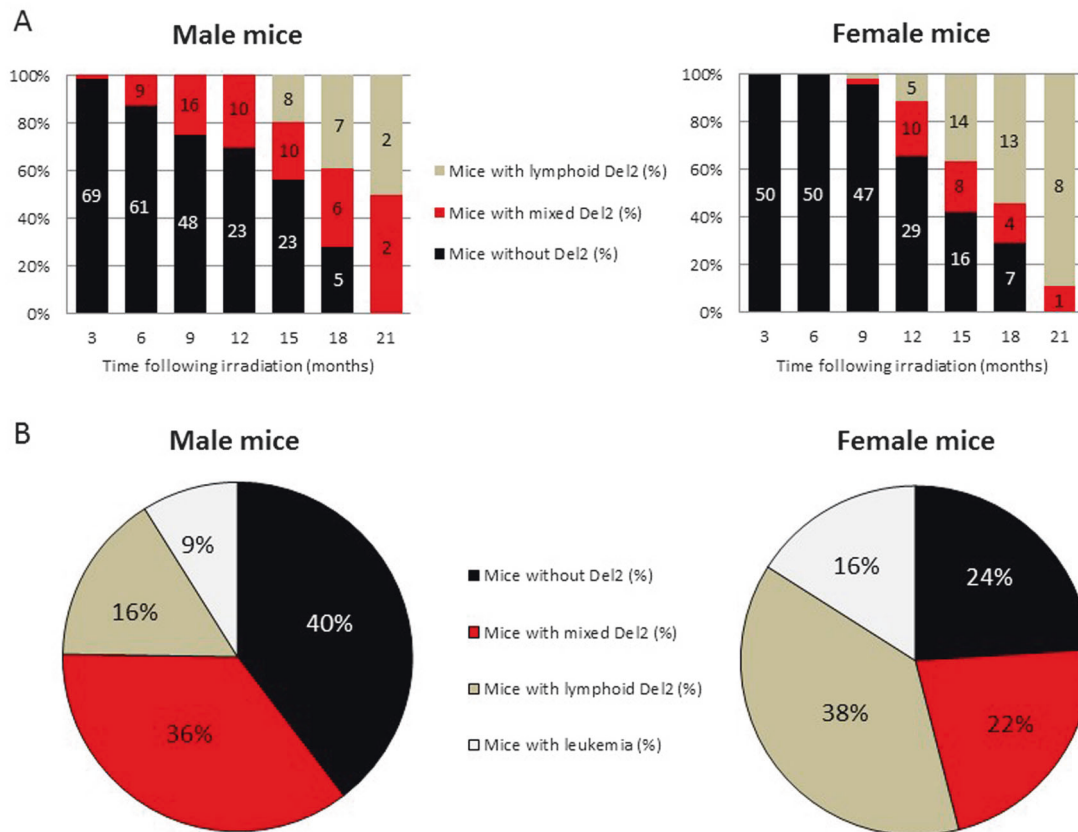


**Fig. 1** Clonal expansion of mCherry– leukocytes in peripheral blood. Blood of irradiated male and female CBA *Sfp11<sup>mCh/GFP</sup>* mice ( $n = 70$  and  $n = 50$ , respectively) was analyzed monthly for mCherry and GFP expression. **a** Percentage of male (left panel) and female (right panel) mice without mCherry loss (black), with both myeloid and lymphoid mCherry loss (red), and with lymphoid mCherry loss (green), detected

in the blood, as a function of time following radiation exposure. Number in the bar reflects the actual number of animals alive at the time point. **b** Percentage of male (left panel) and female (right panel) mice at time of death, diagnosed without mCherry loss (black), with both myeloid and lymphoid mCherry loss (red), with lymphoid mCherry loss (green) or with leukemia (white)

express GFP (i.e., mCherry+GFP–). Myeloid cells (monocytes and granulocytes) require PU.1 for terminal differentiation and maturation, and expressed GFP throughout lifespan (i.e., mCherry+GFP+). Either PU.1 copy (mCherry or GFP) can be deleted during leukemic transformation. However, mCherry loss was used as the ‘lead’ for detection of Del2, allowing GFP to be used as a proxy for PU.1 expression from the remaining copy.

In irradiated animals, clonal expansion of mCherry negative (mCherry–) leukocytes was detected as early as 3 months post-irradiation (Fig. 1a). At 9 months, the percentage of male mice with mCherry– leukocytes was markedly higher compared with females (25% and 4%, respectively), increasing to 70% for both at 18 months (Fig. 1a). Interestingly, the percentage of female mice with clonal expansion of only mCherry– lymphocytes was markedly higher compared with males (54% and 39%, respectively) at 18 months, and increased further by 21 months (Fig. 1a). At death, the percentage of male mice with no mCherry– leukocytes (40% and 24%, respectively), as well as mCherry– mixed myeloid–lymphoid

leukocytes was higher than in females (36% and 22%, respectively; Fig. 1b). Importantly, almost twice as many females were diagnosed with leukemia compared with males (16% and 9%, respectively; Fig. 1b). Irradiated mice with Del2 clonal expansion and unirradiated mice had similar WBC counts ( $6.8 \pm 3.4 \times 10^6/\text{ml}$  and  $7.9 \pm 2.6 \times 10^6/\text{ml}$ , respectively). Only at the time of overt leukemia presentation, WBC counts were increased ( $92.7 \pm 121.8 \times 10^6/\text{ml}$ ).

### Altered PU.1 expression in Del2 leukocytes and hematopoietic progenitors

As most male mice presented with clonal expansion in mCherry– myeloid–lymphoid leukocytes, we hypothesized that Del2 occurred in a very primitive hematopoietic cell type: hematopoietic stem cell (HSC) or multipotent progenitor (MPP). To further characterize the cell of origin, three irradiated male mice with mCherry– myeloid–lymphoid leukocytes were killed. Flow cytometry analysis showed that about 10% Lin– cells were

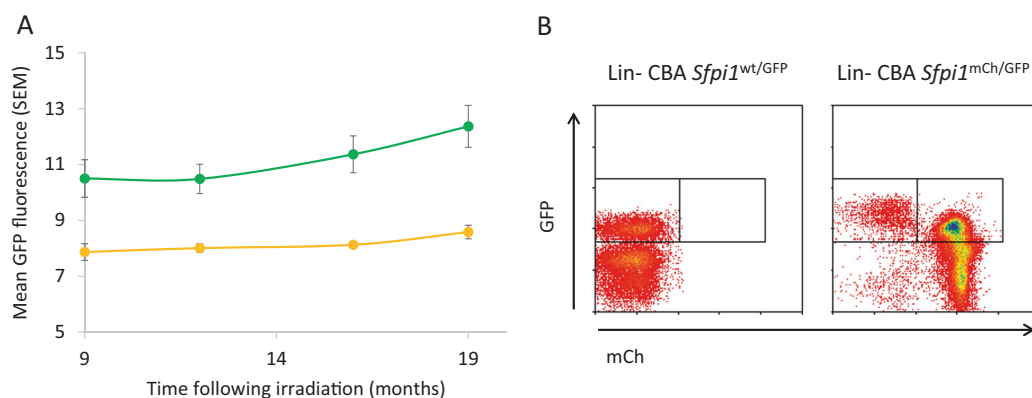


**Fig. 2** GFP expression is upregulated in myeloid leukocytes following Del2. **a** Blood of 8 male mice with clonal expansion in mCherry<sup>+</sup> leukocytes was analyzed for mCherry and GFP expression. Mean GFP fluorescence in mCherry<sup>+</sup> and mCherry<sup>-</sup> granulocytes was compared over time. Error bars indicate SEM. **b** Representative plots of GFP

expression in Lin<sup>-</sup> cells from a sham-irradiated male CBA *Sfpi1*<sup>wt/GFP</sup> mouse, and an irradiated male CBA *Sfpi1*<sup>mCh/GFP</sup> mouse with clonal expansion in mCherry<sup>+</sup> leukocytes (left and right panel, respectively). GFP expression was higher in mCherry<sup>-</sup>Lin<sup>-</sup> cells, compared with mCherry<sup>+</sup>Lin<sup>-</sup> cells

mCherry<sup>-</sup>. Approximately 0.8% of mCherry<sup>-</sup>Lin<sup>-</sup> cells were Sca1<sup>+</sup>cKit<sup>+</sup>, and half of the mCherry<sup>-</sup> LSK fraction was CD48-CD150<sup>+</sup> (i.e., LT-HSCs/MPP1), indicating that these HSCs carried Del2 (Supplementary Figure S2A). Similarly, mCherry<sup>-</sup> myeloid (i.e., mCherry<sup>-</sup>Lin<sup>-</sup>Sca1<sup>-</sup>cKit<sup>+</sup>) and lymphoid progenitors (i.e., mCherry<sup>-</sup>Lin<sup>-</sup>CD127<sup>+</sup>) were identified (Supplementary Figure S2B).

Interestingly, at 18 months, 54% of female mice had clonal expansion of only mCherry<sup>-</sup> lymphocytes. Peripheral blood analysis showed that  $\pm 50\%$  of lymphocytes were mCherry<sup>-</sup>. However, all monocytes and granulocytes were mCherry<sup>+</sup> (Supplementary Figure S3B). BM analysis revealed that only 1.9% of Lin<sup>-</sup> cells were mCherry<sup>-</sup>, compared with 10% in mice with clonal expansion in mCherry<sup>-</sup> myeloid-lymphoid leukocytes. Almost all mCherry<sup>-</sup>Lin<sup>-</sup> cells were Sca1<sup>-</sup>cKit<sup>-</sup> (96%). Although the cell number was low, in these samples no mCherry<sup>-</sup> HSCs or mCherry<sup>-</sup> myeloid progenitors could be identified (Supplementary Figure S3A). However, 11% of mCherry<sup>-</sup>Lin<sup>-</sup> cells expressed CD127, indicating that Del2 most likely occurred in an immature lymphoid cell type (CLP; Supplementary Figure S3B).

To determine PU.1 expression changes on the remaining chr2 after exposure, blood of male mice with clonal expansion of mCherry<sup>-</sup> leukocytes was analyzed for mCherry/GFP expression. When comparing GFP expression between mCherry<sup>-</sup> and mCherry<sup>+</sup> granulocytes, mCherry<sup>-</sup> granulocytes had a markedly higher GFP expression (Fig. 2a). Similarly, GFP expression was higher in mCherry<sup>-</sup>Lin<sup>-</sup> than in mCherry<sup>+</sup>Lin<sup>-</sup> cells (Fig. 2b).

### Exon 5 *Sfpi1* point mutation is solely observed in Del2 hematopoietic cells

There are data suggesting that the *Sfpi1* point mutation most probably leads to complete abolition of PU.1 activity [21,

22]. To identify and quantify the presence of the ‘second’ driving mutation, Lin<sup>-</sup> cells were sorted, based on their mCherry expression, from irradiated male mice with mCherry<sup>-</sup> blood leukocytes. mCherry allele loss occurred specifically in the sorted mCherry<sup>-</sup> population (Fig. 3a). Overall, 16% of mCherry<sup>-</sup>Lin<sup>-</sup> cells in mouse 2 had the characteristic murine rAML C to T substitution, indicating that these mutations are restricted to Del2 Lin<sup>-</sup> cells (Fig. 3b). Point mutations were also analyzed in terminal blood samples. Although not detectable in sham or irradiated CBA *Sfpi1*<sup>mCh/GFP</sup> mice with no mCherry<sup>-</sup> leukocytes, 83% of irradiated mice harboring mCherry<sup>-</sup> clonal expansion showed detectable levels of C to T substitution, linking point mutation occurrence to a prior presence of Del2 (data not shown). Previously, we reported that murine CBA rAML cases without *Sfpi1/PU.1* involvement are rare (<10%; either as chromosome 2 deletion or as *Sfpi1/PU.1* exon 5 mutation), and that within this subset of rAMLs, ~50% of cases has internal tandem duplications (ITDs) within FMS-like tyrosine kinase 3 (*Flt3*) [23]. We have now screened a panel of 134 murine rAML samples and found *Flt3*-ITDs in 3% of the cases, none of them carrying deletions or mutations of *Sfpi1/PU.1*. Interestingly, 2.2% of cases carried a *KRAS* G12 mutation (manuscript in preparation).

### Simultaneous expansion of competing preleukemic clones

At 15 months, one male mouse presented with an unusual clonal expansion of both mCherry<sup>-</sup>/GFP<sup>+</sup> and mCherry<sup>+</sup>/GFP<sup>-</sup> leukocytes, with the point mutation detected in blood leukocytes (6%; Fig. 4a). Three weeks later, the point mutation had increased to 55% in blood (58% in spleen; Fig. 4a) and mCherry<sup>-</sup>Lin<sup>-</sup>/mCherry<sup>+</sup>Lin<sup>-</sup> cells

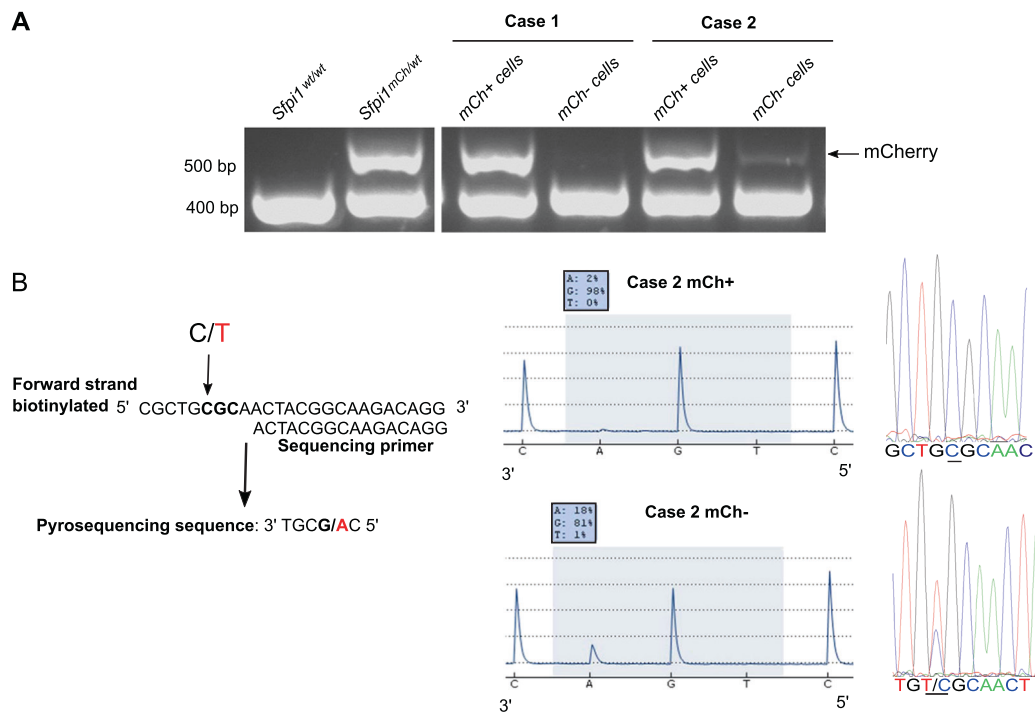


**Fig. 3** Exon 5 *Sfp1* point mutation is solely observed in Del2 hematopoietic cells. **a** Lin<sup>-</sup> cells of male mice were sorted based on mCherry expression. Absence of mCherry in mCherry<sup>-</sup>Lin<sup>-</sup> cells was demonstrated [Rosa26-mCherry allele (510 bp); wild-type allele (383 bp)]. **b** Schematic representation of sequence analyzed by pyrosequencing using sequencing primer complementary to biotinylated

forward strand. Pyrograms depict allele quantification for the first base of the 235th codon of the *Sfp1* gene for mCherry<sup>+</sup>Lin<sup>-</sup> and mCherry<sup>-</sup>Lin<sup>-</sup> cells. Pyrograms indicate the complementary sequence to the forward strand, therefore the % of a indicates the lack or presence of the mutation. Sanger sequencing profiles are presented as well for the same mCherry<sup>+</sup>Lin<sup>-</sup> and mCherry<sup>-</sup>Lin<sup>-</sup> cells

were sorted. Despite being asymptomatic at sacrifice, this mouse had leukemic pathological features, demonstrating that appearance of the point mutation in Del2 blood cells was indicative of a preleukemic mouse at least 1 month prior to AML presentation. Hence, the point mutation occurs late in the leukemogenic process, but presents a rapid increase. Furthermore, both mCherry<sup>-</sup>/GFP<sup>+</sup> and mCherry<sup>+</sup>/GFP<sup>-</sup> leukocytes were detected. A schematic representation of simultaneous expansion of two preleukemic clones (one clone with GFP loss and one with mCherry loss) is presented for this leukemic case (Fig. 4b). *Sfp1* mutation was analyzed in mCherry<sup>+</sup>Lin<sup>-</sup> and mCherry<sup>-</sup>Lin<sup>-</sup> cells, and most mCherry<sup>-</sup> and mCherry<sup>+</sup> cells carried the mutation (63% and 71%, respectively); loss of the GFP allele in mCherry<sup>+</sup>Lin<sup>-</sup> cells was also confirmed (Fig. 4b).

### Dysregulated PU.1 expression upon leukemic progression

We demonstrated that following Del2, PU.1 expression on the remaining homolog is upregulated, indicative of a negative feedback mechanism; with upregulation of the intact chr2 PU.1 promoter being a counter-balancing mechanism. However, in several cases, this feedback

mechanism became dysregulated, possibly when the point mutation occurs, resulting in leukemia development. At 6 months, GFP expression of mCherry<sup>-</sup> granulocytes slightly decreased compared with mCherry<sup>+</sup> granulocytes (Fig. 5a). By 9 months, GFP expression was no longer increased. One month later, mCherry<sup>-</sup> leukocytes percentage had increased further. Shortly thereafter, the mouse presented with outward physical signs of rAML. Although still expressing GFP, 93.5% of cells were mCherry<sup>-</sup>, indicating Rosa26-mCherry chr2 homolog loss. Spleen cell immunophenotyping showed that mCherry<sup>-</sup>GFP<sup>+</sup> cells expressed immaturity cell surface markers (Fig. 5b). Isolated DNA from these cells revealed a TGC sequence. Blood smear showed nucleated cells with blastic appearance while leukemic spleen cells had lost Rosa26-mCherry construct (Fig. 5c).

Notably, most female mice had clonal mCherry<sup>-</sup> lymphocytes expansion. Blood analysis of a female mouse showed that myeloid leukocytes retained mCherry expression at 13 months but 1.9% of lymphocytes were mCherry<sup>-</sup>, increasing further over time. At 17 months, the mouse presented with AML. All mCherry<sup>-</sup> leukemic spleen cells had lost mCherry and GFP expression, indicative of a lymphoid origin. Immunophenotyping showed that cells only expressed CD31 and B220 (Supplementary Figure

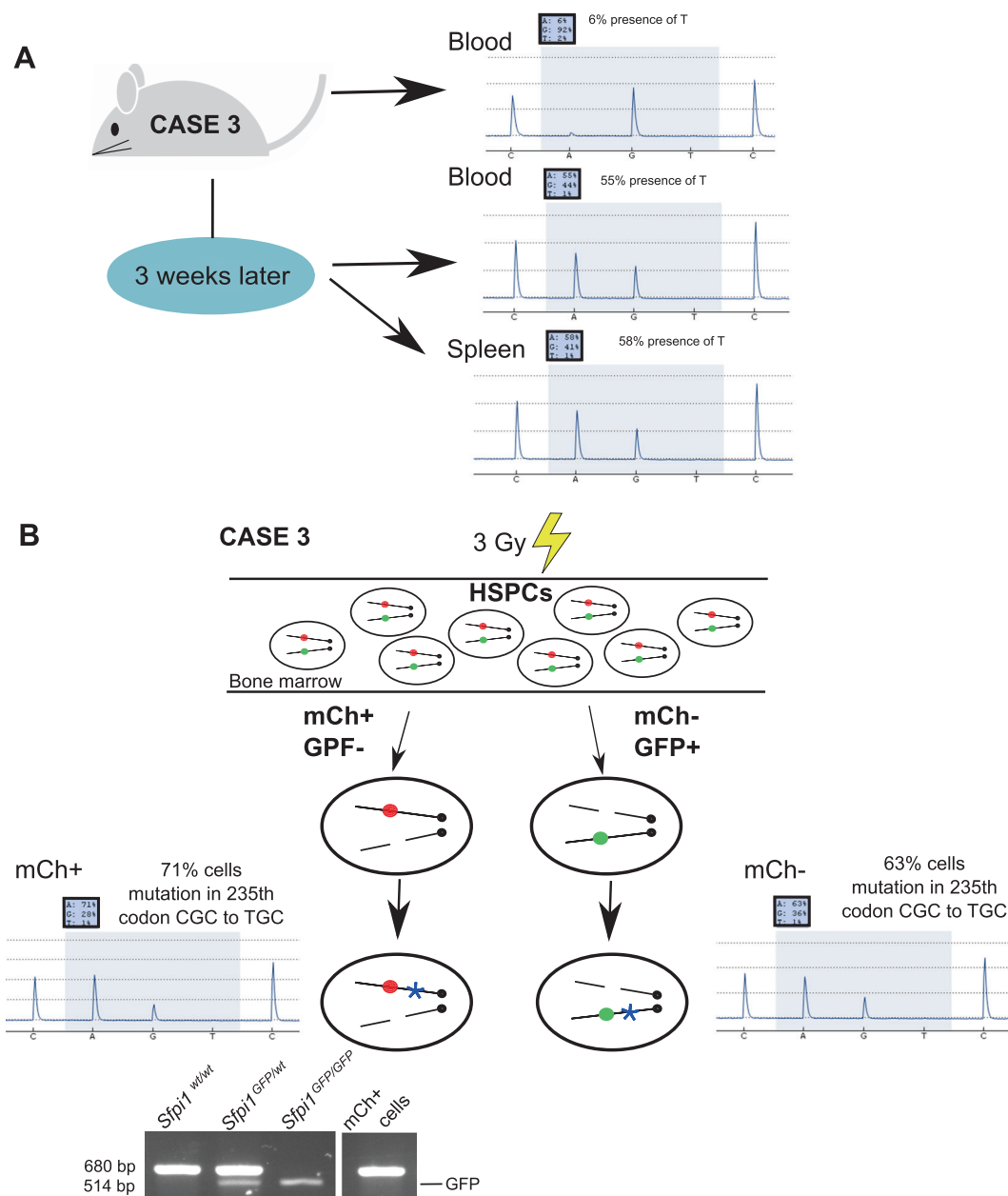


**Fig. 4** Simultaneous expansion of competing preleukemic clones. **a** Blood data of male mouse case 3 with mCherry<sup>-</sup> myeloid and lymphoid leukocytes. The mutation in the 235th codon of the *Sfp1* gene (CGC to TGC) was analyzed at 15 months, and 21 days later at time of sacrifice, by pyrosequencing of blood and spleen. **b** Schematic representation of simultaneous clonal expansion of two preleukemic clones with loss of *Sfp1* alleles (one with GFP and one with mCherry) in this leukemia case. The mutation in the *Sfp1* gene was analyzed in

mCherry<sup>+</sup>Lin<sup>-</sup> and mCherry<sup>-</sup>Lin<sup>-</sup> cells. Pyrograms for allele quantification for the first base of the 235th codon of the *Sfp1* gene are presented for mCherry<sup>+</sup>Lin<sup>-</sup> and mCherry<sup>-</sup>Lin<sup>-</sup> cells. The presence of GFP in mCherry<sup>+</sup>Lin<sup>-</sup> cells was analyzed by PCR. A blue star depicts the presence of the mutation in the 235th codon of the *Sfp1* gene (CGC to TGC), red circle indicates mCherry and green circle GFP

S4A), and no mutation was found on the remaining GFP carrying chr2 homolog. On blood smear, most cells had round nuclei and high nucleus to cytoplasm ratio (Supplementary Figure S4B). Loss of Rosa26-mCherry construct was confirmed. While leukemic cells did not express GFP (i.e., PU.1 downregulation upon commitment towards the

lymphoid lineage), the GFP construct was still detectable by PCR (Supplementary Figure S4C). Seven of the eight female mice were diagnosed with lymphocytic leukemia, while the remaining female was diagnosed with myeloid leukemia, with a much shorter latency compared with male AML cases (5 months and 11 months, respectively).

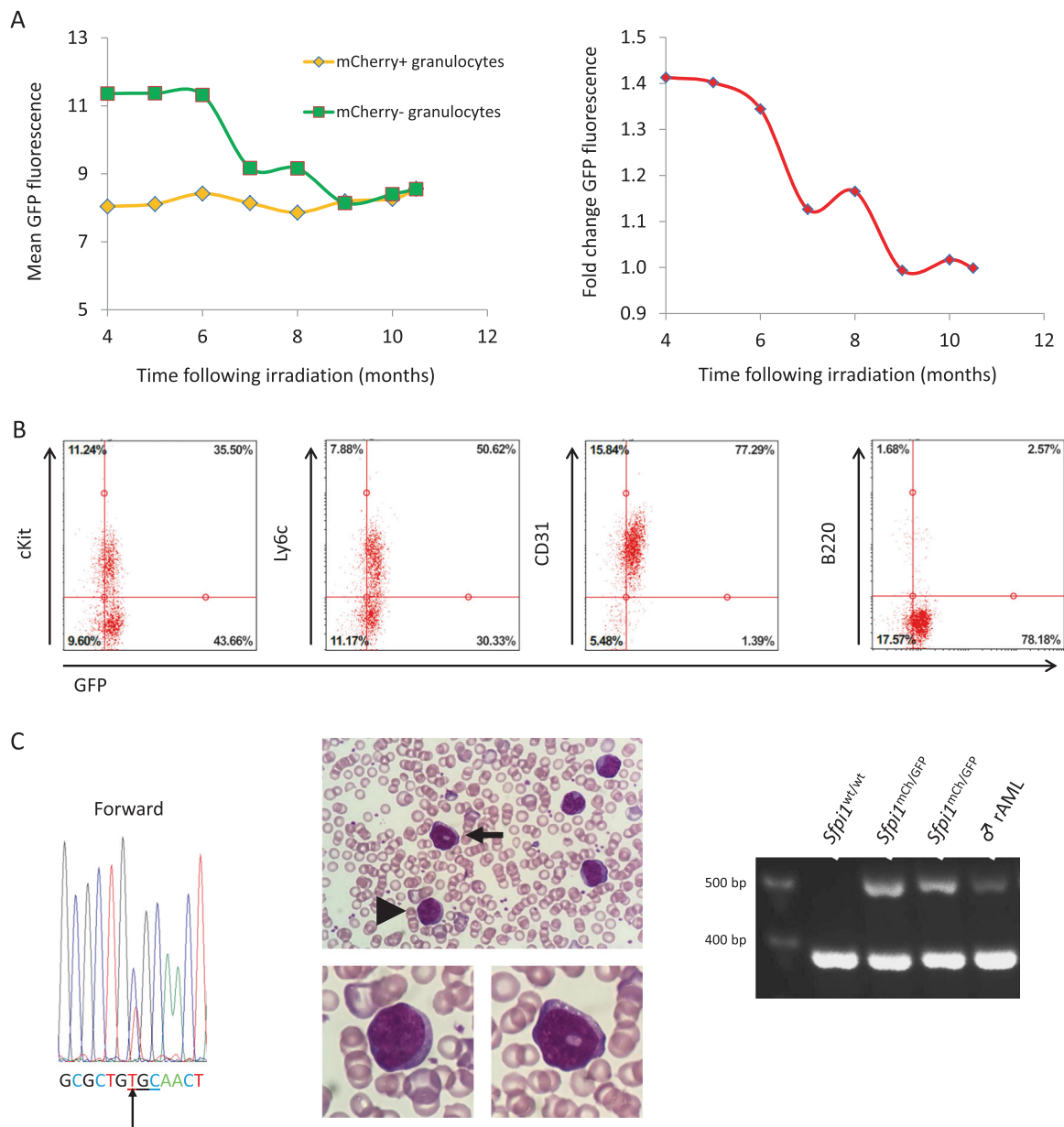


**Fig. 5** Leukemic progression following *Sfpil* dysregulation. **a** At 6 months, GFP expression in mCherry<sup>-</sup> granulocytes of a male mouse had decreased slightly compared with mCherry<sup>-</sup> granulocytes at 4 months. GFP upregulation in mCherry<sup>-</sup> granulocytes decreased further, and at 9 months, GFP expression was no longer different. **b** mCherry<sup>-</sup>GFP<sup>+</sup> spleen cells expressed immaturity cell surface markers. **c** Exon 5 *Sfpil* DNA sequence of the leukemic mouse zoomed in

on the CGC codon known to exhibit the point mutation (arrow indicates the point mutation). Blood smear showed nucleated cells twofold larger than RBCs with a blastic appearance. Confirmation of loss of mCherry allele: control DNA was obtained from a wild-type mouse and 2 sham-irradiated CBA *Sfpil*<sup>mCh/GFP</sup> mice [Rosa26-mCherry allele (510 bp) and wild-type allele (383 bp)]

## Discussion

Using an engineered mouse model, we assessed Del2 occurrence after radiation exposure. A significant number of studies into the cytogenetics of rAML in various inbred mouse strains [24–26] revealed that structurally abnormal chr2—usually consisting of large hemizygous interstitial deletion (i.e., Del2)—occurs in ~90% of rAML cases, and

typically is detectable in 90–100% of the leukemic cells within any sample [27]. It represents by far the most common and consistent chromosomal aberration seen in rAML mouse models. Of the other cytogenetic abnormalities identified in these studies, change in chromosome number is the most frequent. In particular, loss or gain in Y chromosome. More recently, we performed array comparative genomic hybridization (aCGH) at unprecedentedly high

resolution on a unique panel of 79 CBA rAMLs [27]. Besides the characteristic Del2, small deletions were observed on chrs 3, 4, 5, 6, 11, and 16 in individual cases, but importantly no consistent event was identified.

At 9 months after radiation exposure, 25% of males presented with mCherry<sup>−</sup> leukocytes, in line with previously reported percentages in irradiated mice with BM Del2 clones, detected with cytogenetic methods [14]. All these male mice had mCherry loss in both myeloid and lymphoid lineages, indicative of a primitive hematopoietic cell type (HSC or MPP1). Using SLAM markers, we identified mCherry<sup>−</sup> HSCs (LSK CD48<sup>−</sup>CD150<sup>+</sup>) [28] in mice with mixed lineage mCherry<sup>−</sup> clonal expansion in blood. These mice had mCherry<sup>−</sup> myeloid and lymphoid progenitors, based on differential CD127 expression in these cells [29, 30], indicating that Del2 HSCs gave rise to mCherry<sup>−</sup> daughter HSCs as well as mCherry<sup>−</sup> lineage-committed progeny. At 15 months, 8 out of 18 males presented with lymphoid lineage-only mCherry<sup>−</sup> cells, indicating that in these mice Del2 likely occurred in a hematopoietic cell-like a CLP giving rise to lymphoid progeny specifically.

We assessed PU.1 expression from the remaining chr2 homolog in mice with mCherry<sup>−</sup> leukocytes (GFP as reporter for PU.1 transcription) [27, 31]. GFP expression in mCherry<sup>−</sup> myelocytes was 1.4-fold higher compared with mCherry<sup>+</sup>myelocytes. It can be directly attributed to an increased PU.1 promoter activity through PU.1 autoregulation to compensate the loss of the second allele. It was previously reported that both URE and *Sfp1* proximal promoter have binding sites for PU.1 itself [32–34]. Here we report that during leukemogenesis, autoregulation of PU.1 was observed in mCherry<sup>−</sup> Lin<sup>−</sup> cells. This autoregulation becomes dysregulated, resulting in GFP expression decreasing to the level of mCherry<sup>+</sup>leukocytes. In these cases, immunophenotyping showed immature phenotypes consistent with myeloid leukemia. We also confirmed that the remaining *Sfp1* copy carried a point mutation replacing arginine 235 with cysteine (the most common C to T substitution in murine rAMLs) [35] probably impairing transcriptional autoregulation. Our experimental observations are consistent with a two-hit model of murine radiation leukemogenesis in which the first irreversible mutational hit (deletion of one *Sfp1* copy) results in preleukemic cells with growth advantage. Subsequently, they acquire a second mutational hit (point mutation in the remaining *Sfp1*), leading to full malignancy, clonal expansion and leukemia [13].

It could be hypothesized that the point mutation occurs when the GFP levels return to ‘normal’ levels (i.e., equal to mCherry<sup>+</sup> leukocytes), linking point mutation occurrence with loss of PU.1 autoregulation. Data obtained from terminal blood samples of irradiated mice revealed that 83%

of mice had mutated cells. In contrast, the point mutation couldn’t be detected neither in sham-irradiated mice nor irradiated mice without mCherry<sup>−</sup> leukocytes. In addition, point mutations were exclusively detected in the BM mCherry<sup>−</sup>Lin<sup>−</sup> cell fraction of mice with mCherry<sup>−</sup> leukocytes. Most importantly, these observations link, for the first time, the occurrence of the point mutation to a prior presence of Del2. The leukemic case described with two competing preleukemic clones provides evidence of how rapid the leukemic progression occurs following acquisition of the second hit (6% to 55% in merely three weeks). To the best of our knowledge, only one study so far reported an alternative mutation occurring in a mutually exclusive way with *Sfp1/PU.1* [23]. RFLP and sequencing analysis revealed in a subset of rAMLs the presence of *Flt3*-ITDs (one of the most frequent mutations in human AMLs [36]). These ITDs are similar to those seen in human AML cases and the mutual exclusion with *Sfp1/PU.1* mutations suggests that *Flt3* mutations are driver mutations in these rare rAML cases. We have now screened a panel of 134 CBA rAML samples and found *Flt3*-ITDs in 3% of the cases (unpublished data). Although this is clearly a minor pathway, it represents the only significant alternative pathway to rAML identified so far in this mouse model with a direct link to human AML. In addition, we recently found a few rAML with leukemic cells carrying a *KRAS* mutation concomitantly to Del2 and *Sfp1* mutations (data not shown), none of them with additional *Flt3*-ITDs, suggesting different leukemogenic pathways.

Overall male rAML incidence was 9% with an average latency of 11 months, consistent with previous work in male CBA mice [8, 16, 37]. One in three females had mCherry<sup>−</sup> lymphoid but not myeloid leukocytes at 12 months. The mean leukemic latency was similar to males (i.e., 13 and 11 months, respectively;  $P = 0.49$ ). All but one male leukemia cases were categorized as myeloid leukemia. In contrast, 7 out of 8 female leukemia cases were categorized as lymphoid leukemia. Previous work reported AML incidences higher among irradiated males than females. [16, 38–40] Our data suggest that a gender-specific hematopoietic cell subpopulation leads to clonal expansion (HSC/MPP1 vs CLP). Interestingly, PU.1-knockout in lymphoid progenitors does not alter B-cell-maturation or proliferation [41], possibly explaining the mature B-cell phenotype in our female AMLs (i.e., B220 expression). On the other hand, PU.1-knockout in myeloid progenitors inhibits their maturation but not their proliferation [41], consistent with the immature myeloid phenotype observed in our male AMLs. However, we assume that all lineages are prone to Del2 to the same extent, but that cell intrinsic or external factors promoting their expansion, may be gender-specific.

An intrinsic gender-specific radiosensitivity is highly unlikely, and albeit not yet well understood, sex hormones



might have a pivotal role. For example, castration does not affect rAML incidence, whereas ovariectomy results in a twofold increase [42]. Interestingly, gonadectomy does not alter leukemia incidence in unexposed mice [42]. It was also shown that estrogen binding to its receptor enhanced HSC self-renewal by upregulation of cell-cycle genes [43]. Follow-up of atomic bomb survivors reported that female AML baseline rate is ~40% of that for men who displayed a more rapid increased AML incidence rate with attained age [1]. In conclusion, we propose, based on our experimental data, a model with gender dependent leukemic pathways (Supplementary Figure S5). Our study provides novel insights into (radiation) leukemogenesis, and the model should enable further deciphering of this complex multistep process.

**Acknowledgements** The transgenic reporter gene model C57BL/6 *Sfp1*<sup>GFP/GFP</sup> was generously provided by Professor Stephen Nutt from the Walter and Eliza Hall Institute in Melbourne, Australia.

### Compliance with ethical standards

**Conflict of interest** The authors declare that they have no conflict of interest.

**Open Access** This article is licensed under a Creative Commons Attribution 4.0 International License, which permits use, sharing, adaptation, distribution and reproduction in any medium or format, as long as you give appropriate credit to the original author(s) and the source, provide a link to the Creative Commons license, and indicate if changes were made. The images or other third party material in this article are included in the article's Creative Commons license, unless indicated otherwise in a credit line to the material. If material is not included in the article's Creative Commons license and your intended use is not permitted by statutory regulation or exceeds the permitted use, you will need to obtain permission directly from the copyright holder. To view a copy of this license, visit <http://creativecommons.org/licenses/by/4.0/>

### References

- Hsu W-L, Preston DL, Soda M, Sugiyama H, Funamoto S, Kodama K, et al. The incidence of leukemia, lymphoma and multiple myeloma among atomic bomb survivors: 1950-2001. *Radiat Res.* 2013;179:361-82.
- Yu G-P, Schantz SP, Neugut AI, Zhang Z-F. Incidences and trends of second cancers in female breast cancer patients: a fixed inception cohort-based analysis (United States). *Cancer Causes Control.* 2006;17:411-20.
- Kaplan H, Malmgren J, DeRoos A. Increased risk of MDS/AML post radiation treatment for breast cancer: analysis of SEER data 2001-8. *J Clin Oncol.* 2012;30:abstr 6560.
- Travis LB. Treatment-associated leukemia following testicular cancer. *J Natl Cancer Inst.* 2000;92:1165-71.
- Wright JD, St. Clair CM, Deutsch I, Burke WM, Gorrochurn P, Sun X, et al. Pelvic radiotherapy and the risk of secondary leukemia and multiple myeloma. *Cancer.* 2010;116:2486-92. NA-NA
- Radvoyevitch T, Sachs RK, Gale RP, Molenaar RJ, Brenner DJ, Hill BT, et al. Defining AML and MDS second cancer risk dynamics after diagnoses of first cancers treated or not with radiation. *Leukemia.* 2016;30:285-94.
- Shlush LI, Zandi S, Mitchell A, Chen WC, Brandwein JM, Gupta V, et al. Identification of pre-leukaemic haematopoietic stem cells in acute leukaemia. *Nature.* 2014;506:328-33.
- Major IR. Induction of myeloid leukaemia by whole-body single exposure of CBA male mice to X-rays. *Br J Cancer.* 1979;40:903-13.
- Verbiest T, Bouffler S, Nutt SL, Badie C. PU.1 downregulation in murine radiation-induced acute myeloid leukaemia (AML): from molecular mechanism to human AML. *Carcinogenesis.* 2015;36:413-9.
- Rithidech KN, Bond VP, Cronkite EP, Thompson MH. A specific chromosomal deletion in murine leukemic cells induced by radiation with different qualities. *Exp Hematol.* 1993;21:427-31.
- Alexander BJ, Rasko JE, Morahan G, Cook WD. Gene deletion explains both in vivo and in vitro generated chromosome 2 aberrations associated with murine myeloid leukemia. *Leukemia.* 1995;9:2009-15.
- Cook WD. PU.1 is a suppressor of myeloid leukemia, inactivated in mice by gene deletion and mutation of its DNA binding domain. *Blood.* 2004;104:3437-44.
- Dekkers F, Bijwaard H, Bouffler S, Ellender M, Huiskamp R, Kowalczuk C, et al. A two-mutation model of radiation-induced acute myeloid leukemia using historical mouse data. *Radiat Environ Biophys.* 2011;50:37-45.
- Bouffler SD, Meijne EI, Morris DJ, Papworth D. Chromosome 2 hypersensitivity and clonal development in murine radiation acute myeloid leukaemia. *Int J Radiat Biol.* 1997;72:181-9.
- Olme C-H, Brown N, Finnon R, Bouffler SD, Badie C. Frequency of acute myeloid leukaemia-associated mouse chromosome 2 deletions in X-ray exposed immature haematopoietic progenitors and stem cells. *Mutat Res Toxicol Environ Mutagen.* 2013;756:119-26.
- Olme C-H, Finnon R, Brown N, Kabacik S, Bouffler SD, Badie C. Live cell detection of chromosome 2 deletion and *Sfp1*/PU.1 loss in radiation-induced mouse acute myeloid leukaemia. *Leuk Res.* 2013;37:1374-82.
- Verbiest T, Finnon R, Brown N, Finnon P, Bouffler S, Badie C. NOD scid gamma mice are permissive to allogeneic HSC transplantation without prior conditioning. *Int J Mol Sci.* 2016;17:1850.
- Kogan SC, Ward JM, Anver MR, Berman JJ, Brayton C, Cardiff RD, et al. Bethesda proposals for classification of nonlymphoid hematopoietic neoplasms in mice. *Blood.* 2002;100:238-45.
- Brown NL, Finnon R, Bulman RA, Finnon P, Moody J, Bouffler SD, et al. *Sfp1*/PU.1 mutations in mouse radiation-induced acute myeloid leukaemias affect mRNA and protein abundance and associate with disrupted transcription. *Leuk Res.* 2011;35:126-32.
- Peng Y, Brown N, Finnon R, Warner CL, Liu X, Genik PC, et al. Radiation leukemogenesis in mice: loss of *PU.1* on chromosome 2 in CBA and C57BL/6 mice after irradiation with 1 GeV/nucleon <sup>56</sup>Fe ions, X rays or  $\gamma$  rays. Part I. Experimental observations. *Radiat Res.* 2009;171:474-83.
- Genik PC, Vyazunova I, Steffen LS, Bacher JW, Bielefeldt-Ohmann H, McKercher S, et al. Leukemogenesis in heterozygous *PU.1* knockout mice. *Radiat Res.* 2014;182:310-5.
- Metcalfe D, Dakic A, Mifsud S, Di Rago L, Wu L, Nutt S. Inactivation of PU.1 in adult mice leads to the development of myeloid leukemia. *Proc Natl Acad Sci USA.* 2006;103:1486-91.
- Finnon R, Brown N, Moody J, Badie C, Olme CH, Huiskamp R, et al. *Flt3*-ITD mutations in a mouse model of radiation-induced acute myeloid leukaemia. *Leukemia.* 2012;26:1445-6.
- Hayata I, Seki M, Yoshida K, Hirashima K, Sado T, Yamagiwa J, et al. Chromosomal aberrations observed in 52 mouse myeloid leukemias. *Cancer Res.* 1983;43:367-73.

25. Bouffler SD, Meijne EI, Huiskamp R, Cox R. Chromosomal abnormalities in neutron-induced acute myeloid leukemias in CBA/H mice. *Radiat Res.* 1996;146:349–52.
26. Clark DJ, Meijne EI, Bouffler SD, Huiskamp R, Skidmore CJ, Cox R, et al. Microsatellite analysis of recurrent chromosome 2 deletions in acute myeloid leukaemia induced by radiation in F1 hybrid mice. *Genes Chromosomes Cancer.* 1996;16:238–46.
27. Brown N, Finnon R, Manning G, Bouffler S, Badie C. Influence of radiation quality on mouse chromosome 2 deletions in radiation-induced acute myeloid leukaemia. *Mutat Res Genet Toxicol Environ Mutagen.* 2015;793:48–54.
28. Kiel MJ, Yilmaz OH, Iwashita T, Yilmaz OH, Terhorst C, Morrison SJ. SLAM family receptors distinguish hematopoietic stem and progenitor cells and reveal endothelial niches for stem cells. *Cell.* 2005;121:1109–21.
29. Kondo M, Weissman IL, Akashi K. Identification of clonogenic common lymphoid progenitors in mouse bone marrow. *Cell.* 1997;91:661–72.
30. Akashi K, Traver D, Miyamoto T, Weissman IL. A clonogenic common myeloid progenitor that gives rise to all myeloid lineages. *Nature.* 2000;404:193–7.
31. Nutt SL, Metcalf D, D'Amico A, Polli M, Wu L. Dynamic regulation of PU.1 expression in multipotent hematopoietic progenitors. *J Exp Med.* 2005;201:221–31.
32. Chen H, Ray-Gallet D, Zhang P, Hetherington CJ, Gonzalez DA, Zhang DE, et al. PU.1 (Spi-1) autoregulates its expression in myeloid cells. *Oncogene.* 1995;11:1549–60.
33. Okuno Y, Huang G, Rosenbauer F, Evans EK, Radoomska HS, Iwasaki H, et al. Potential autoregulation of transcription factor PU.1 by an upstream regulatory element. *Mol Cell Biol.* 2005;25:2832–45.
34. Staber PB, Zhang P, Ye M, Welner RS, Nombela-Arrieta C, Bach C, et al. Sustained PU.1 levels balance cell-cycle regulators to prevent exhaustion of adult hematopoietic stem cells. *Mol Cell.* 2013;49:934–46.
35. Steffen LS, Bacher JW, Peng Y, Le PN, Ding L-H, Genik PC, et al. Molecular characterisation of murine acute myeloid leukaemia induced by 56Fe ion and 137Cs gamma ray irradiation. *Mutagenesis.* 2013;28:71–79.
36. Welch JS, Ley TJ, Link DC, Miller CA, Larson DE, Koboldt DC, et al. The origin and evolution of mutations in acute myeloid leukemia. *Cell.* 2012;150:264–78.
37. Weil MM, Bedford JS, Bielefeldt-Ohmann H, Ray FA, Genik PC, Ehrhart EJ, et al. Incidence of acute myeloid leukemia and hepatocellular carcinoma in mice irradiated with 1 GeV/nucleon (56)Fe ions. *Radiat Res.* 2009;172:213–9.
38. Di Majo V, Coppola M, Rebessi S, Saran A, Pazzaglia S, Pariset L, et al. The influence of sex on life shortening and tumor induction in CBA/Cne mice exposed to X rays or fission neutrons. *Radiat Res.* 1996;146:81–87.
39. Yoshida K, Nemoto K, Nishimura M, Seki M. Exacerbating factors of radiation-induced myeloid leukemogenesis. *Leuk Res.* 1993;17:437–40.
40. Upton AC, Odell TT, Sniffen EP. Influence of age at time of irradiation on induction of leukemia and ovarian tumors in RF mice. *Exp Biol Med.* 1960;104:769–72.
41. Iwasaki H, Somoza C, Shigematsu H, Duprez EA, Iwasaki-Arai J, Mizuno S-I, et al. Distinctive and indispensable roles of PU.1 in maintenance of hematopoietic stem cells and their differentiation. *Blood.* 2005;106:1590–1600.
42. Upton AC. Studies on the mechanism of leukaemogenesis by ionizing radiation. In: Wolstenholme GEW, O'Connor M, editors. *Novartis Foundation symposia.* Chichester, UK: John Wiley & Sons, Ltd.; 2008. pp. 249–73.
43. Nakada D, Oguro H, Levi BP, Ryan N, Kitano A, Saitoh Y, et al. Oestrogen increases haematopoietic stem-cell self-renewal in females and during pregnancy. *Nature.* 2014;505:555–8.